Bull. Mater. Sci. (2020) 43:172
https://doi.org/10.1007/s12034-020-02089-4

Design of cationic amphiphiles for generating self-assembled soft nanostructures, micelles and hydrogels

OMPRAKASH SUNNAPU[1,2], PRIUSHA RAVIPATI[1], PREETHEM SRINATH[1], SANJEEB KALITA[1], PRATIKSHA P BHAT[1], S R HARSHITHA[1], KARUPPANNAN SEKAR[2], PRAVEEN KUMAR VEMULA[1] and MANOHAR MAHATO[1,*]

[1]Institute for Stem Cell Science and Regenerative Medicine (inStem), GKVK Campus, Bengaluru 560065, India
[2]Department of Chemistry, Anna University, University College of Engineering, Dindigul 624622, India
*Author for correspondence (manohar113@gmail.com)

MS received 19 August 2019; accepted 20 December 2019; published online 29 July 2020

Abstract. Design of amphiphiles to develop robust self-assembled soft nanomaterials, such as micelles and hydrogels is an interesting subject. A series of cationic amphiphilic compounds were synthesized comprising 1-ethoxy (3-pentadecyl) benzene as the hydrophobic tail. The second carbon of ethoxy was linked to quaternary head groups (trimethyl ammonium bromide (PEA), triethyl ammonium bromide (PETE), pyridinium bromide (PEPy), *N*-methyl morpholino bromide (PENM), *N*-methyl piperidine bromide (PENP)). Inclusion of benzene ring leads to a significant decrease in critical micellar concentration (CMC) as compared to other cationic surfactants, such as cetyl trimethyl ammonium bromide (CTAB). Interestingly, at higher concentration, these cationic amphiphiles were forming soft hydrogels with critical gelation concentration (CGC) from 3 to 10% (w/v). The small-angle X-ray scattering (SAXS) analysis of xerogel revealed the formation of self-assembled lamellar patterns of molecules. Further, the morphology of xerogels were also seen under a scanning electron microscope (SEM) which correlates with SAXS data. The SAXS and SEM data confirms the formation of worm-like micellar structures and entangle themselves to form a hydrogel. The cytotoxicity assay was done on HDFA, HeLa and HEK cell lines, haemolysis assay showed better haemocompatibility than CTAB. The synthesized surfactants exhibited up to 3-fold higher solubilization capability against hydrophobic molecules than CTAB.

Keywords. Cationic surfactant; worm-like micelles; hydrogels; viscoelasticity; xerogels; supramolecular interactions.

1. Introduction

Surfactants have always been the molecules of interest in cosmetics, pharmaceutics, chemical engineering field due to their emulsifying, solubilizing, anti-fogging, deinking and many more properties [1]. There has been extensive research done on limitless designing, modification in the hydrophobic chain and hydrophilic head group, which resulted in gemini surfactant, multi-chain surfactant, multi-head group surfactant and bola-amphiphilic surfactant [2–5]. Moreover, the aggregation behaviour of surfactants with respect to salinity, pH, surfactant concentration and temperature have been thoroughly studied [6]. These studies coined the term 'worm-like micelles', which defines the characteristic behaviour of surfactant above their critical micellar concentration (CMC) values and show viscoelasticity in aqueous solution [7]. The worm-like micelles form rod-like structure and entangle themselves to form gel-like structures [8]. Therefore, completely mimicking the polymers and act like living polymer in the solution [8]. The worm-like micellar (WM) system have replaced polymers in the oil extraction industry where they are used as 'fracking fluids' [9]. As cross-linked polymer got stuck to the fractured areas and inhibit the hydraulic conductivity, but in case of WM, they show gel-like fluid, which carries the sand (the proppant) to the fractured bedrock site. Due to the high temperature at fractured site, WM gets changed into spherical micelles and leave the sand behind the fractured site. The cationic surfactants are also used as drag reducing agents particularly, because they do not precipitate in the presence of calcium and magnesium salts, unlike anionic surfactant [10]. Moreover, stimuli-responsive worm-like micelles have also been explored to have an application in the field of nanobiotechnology [6].

However, to form worm-like micelles from mono-tail surfactant, various salts including aromatic salts (like sodium salicylate), zwitterionic surfactant, counter surfactant have been employed [11,12]. There are very few reports, which show the formation of worm-like micelles followed by hydrogel formation using mono-tail surfactant in the absence of any kind of initiator, such as salts and helper surfactants. The stability of the self-assembled aggregates depends on non-covalent interactions between the individual molecule, which predominantly decides the CMC value of surfactant. Apart from hydrophobic interactions from alkyl chain, aromatic residues also been incorporated to induce π–π stacking interaction as well to form much stable aggregates and reduce

CMC. This phenomenon has been proved in a study where phenyl ring is systematically placed in hydrophobic chain, and CMC value also decreases significantly [13]. The surfactant with substituted aromatic group apart from para-position has not been studied, which can provide a better understanding of self-assembled structure with position isomers.

In this study, we have designed a series of cationic amphiphiles using the following design criteria. A hydrophobic pentadecyl chain was directly connected to phenol at *meta* position, and different cationic head groups were connected to the phenoxy group through ethylene linker (scheme 1). Pentadecyl chain provides hydrophobic interactions while aromatic group facilitates π–π interactions, together with polar head groups, they can facilitate robust self-assembly in aqueous/buffer media. Self-assembly of these amphiphiles has been investigated systematically. The cationic amphiphiles have lower CMC than 1 mM, and reduced even more in the presence of phosphate buffer solution (PBS) due to salting-out effect [14]. At higher concentration, these amphiphiles were able to form worm-like micelles followed by viscoelastic hydrogels. The hydrogel characteristics were determined by rheological studies, and the molecular arrangement was found by small angle X-ray scattering (SAXS) studies. The SAXS studies confirm the lamellar assembly of molecules, which resulted from worm-like rods and entangles to form branched structures. The morphology of xerogels was evaluated by using scanning electron microscope (SEM) and micrographs showed complete correlation with SAXS data and proving the formation of worm-like micelles. Further, the cationic amphiphiles were assessed for their biocompatibility and solubilization of curcumin as a model drug, which is poorly water-soluble molecule.

2. Experimental

2.1 *Synthesis of cationic amphiphile*

2.1a *Synthesis of 1-(2-bromoethoxy)-3-pentadecyl benzene [**1**]*: 3-pentadecyl phenol (25 g), potassium hydroxide pellets (5.5 g, 1.2 eq.) and 1,2-dibromoethane (35.7 ml, 5 eq.) was taken in a round bottomed flask. The mixture was refluxed for 24 h, and completion of the reaction was monitored over thin layer chromatography (TLC) plate. After completion of the reaction, the reaction mixture was concentrated using rotavapor. Further, ethyl acetate (400 ml) was added to the concentrated reaction mixture, and the organic phase was triturated with distilled water three times, followed by two brine washes. The organic phase was dried over anhydrous sodium sulphate, and the compound was recovered after removing ethyl acetate through rotavapor. The compound was eluted over silica column chromatography using hexane:ethyl acetate (98:2) as mobile phase with 85% yield (28.75 g).

^{1}H-NMR in $CDCl_3$ (600 MHz), δ (ppm): 0.9 (3H, t, $–CH_3$), 1.28 (24H, m, alkyl chain), 2.6 (2H, t, $–CH_2$, benzyl), 3.6 (2H, t, $–CH_2–Br$), 4.3 (2H, t, $–CH_2–O–$), 6.7–7.2 (4H, m, aryl).

2.1b *Synthesis of N,N,N-trimethyl-2-(3-pentadecylphenoxy) ethan-1-aminium bromide [PEA, **2a**]*: The compound **1** (3 g) and potassium carbonate (1.5 g) were added to tetrahydrofuran (15 ml) in pressure sealed tube. To the reaction mixture, 30% trimethylamine aqueous solution (20 ml) was added and heated at 80°C for 48 h with constant stirring. The completion of the reaction was monitored over TLC, and after completion of the reaction, the reaction mixture was transferred to round bottomed flask and the reaction mixture was concentrated till dryness. To the dried reaction mixture, 20 ml of chloroform:methanol (8:2) was added to precipitate the salts and dissolve the quaternary ammonium salt (**2a**). Further, the organic phase was removed using rotavapor and kept the obtained compound in a vacuum for overnight. The dried compound was precipitated by addition of hexane, and the desired compound was filtered and dried under vacuum with 80% yield (2.7 g).

^{1}H-NMR in $CDCl_3$ (600 MHz), δ (ppm): 0.9 (3H, t, $–CH_3$), 1.28 (24H, m, alkyl chain), 2.6 (2H, t, $–CH_2$, benzyl), 3.5 (9H, s, $–N^+(CH_3)_3$), 4.3 (2H, t, $–CH_2–N^+(CH_3)_3$), 4.5 (2H, t, $–CH_2–O–$), 6.7–7.2 (4H, m, aryl).

Mass (m/z): 390 [M^+].

2.1c *Synthesis of N,N,N-triethyl-2-(3-pentadecylphenoxy) ethan-1-aminium bromide [PETE, **2b**]*: The compound **1** (3 g) and triethyl amine (5 ml) was added to sealed pressure tube and stirred for 48 h at 80°C. After completion of the reaction as monitored over TLC, the reaction mixture was transferred to a 250 ml conical flask, and hexane (100 ml) was added to it. The obtained precipitate was filtered, washed thoroughly with hexane, and dried under a vacuum to get the compound (3 g, ~80% yield).

^{1}H-NMR in $CDCl_3$ (600 MHz), δ (ppm): 0.9 (3H, t, $–CH_3$), 1.28 (24H,m, alkyl chain), 2.6 (2H, t, $–CH_2$, benzyl), 1.5 (9H, t, $–N^+(CH_2\mathbf{CH_3})_3$), 3.6 (6H, q, $–N^+(\mathbf{CH_2}CH_3)_3$), 4.3 (2H, t, $–CH_2–N^+(CH_3)_3$), 4.5 (2H, t, $–CH_2–O–$), 6.7–7.2 (4H, m, aryl).

Mass (m/z): 432 [M^+].

2.1d *Synthesis of 1-(2-(3-pentadecylphenoxy)ethyl)pyridin-1-ium bromide [PEPy, **2c**]*: The compound **1** (3 g) and pyridine (5 ml) was added to sealed pressure tube and stirred for 48 h at 90°C. After completion of the reaction as monitored over TLC, the reaction mixture was transferred to a round bottomed flask, and excess of pyridine was evaporated on rotavapor. The compound was precipitated with diethyl ether, filtered and followed by subsequent washing using diethyl ether. The compound was dried under a vacuum and recovered with ~80% yield (2.86 g).

^{1}H-NMR in $CDCl_3$ (600 MHz), δ (ppm): 0.9 (3H, t, $–CH_3$), 1.28 (24H, m, alkyl chain), 2.6 (2H, t, $–CH_2$, benzyl), 4.3 (2H,

t, $-CH_2-O-$), 5.57 (2H, t, $-CH_2-$pyridinium), 6.7–7.2 (4H, m, aryl), 8.1 (2H, m, pyridinium), 8.5 (1H, t, pyridinium), 9.6 (2H, d, pyridinium).

Mass (m/z): 410 [M^+].

2.1e *Synthesis of 4-methyl-4-(2-(3-pentadecylphenoxy) ethyl) morpholin-4-ium bromide [PENM, **2d**]*: The procedure for synthesizing **2d** was followed the same as **2b** by replacing *N*-methyl morpholino with triethyl amine. The compound was precipitated in diethyl ether and dried under a vacuum in ~80% yield (2.9 g).

^{1}H-NMR in $CDCl_3$ (600 MHz), δ (ppm): 0.9 (3H, t, $-CH_3$), 1.28 (24H, m, alkyl chain), 2.6 (2H, t, $-CH_2$, benzyl), 3.67 (3H, s, $-N^+(CH_3)$), 3.9 (4H, m, $-C\mathbf{H_2}-O-C\mathbf{H_2}$), 4.1 (4H, m, $-C\mathbf{H_2}-N^+(CH_3)-C\mathbf{H_2}$), 4.4 (2H, t, $-C\mathbf{H_2}-N^+(CH_3)$), 4.5 (2H, t, $-C\mathbf{H_2}-$O–aryl), 6.7–7.2 (4H, m, aryl).

Mass (m/z): 432 [M^+].

2.1f *Synthesis of 1-methyl-1-(2-(3-pentadecylphenoxy)ethyl) piperidin-1-ium bromide [PENP, **2e**]*: The procedure for synthesizing **2e** was followed the same as **2b** by replacing *N*-methyl piperidine with triethyl amine. The compound was precipitated in diethyl ether and dried under a vacuum in ~80% yield (2.9 g).

^{1}H-NMR in $CDCl_3$ (600 MHz), δ (ppm): 0.9 (3H, t, $-CH_3$), 1.28 (24H, m, alkyl chain), 1.8–2.0 (6H, m, $-CH_2-(C\mathbf{H_2})_3-CH_2$), 2.6 (2H, t, $-CH_2$, benzyl), 3.51 (3H, s, $-N^+(CH_3)$), 3.7–3.9 (4H, m, $-C\mathbf{H_2}-N^+(CH_3)-C\mathbf{H_2}$), 4.4 (2H, t, $-C\mathbf{H_2}-N^+(CH_3)$), 4.5 (2H, t, $-C\mathbf{H_2}-$O–aryl), 6.7–7.2 (4H, m, aryl).

Mass (m/z): 430 [M^+].

2.2 *CMC determination*

To determine the CMC of cationic surfactant molecule, pyrene was used as luminescence probe, which is extremely sensitive towards hydrophobic environment around it. Briefly, 0.5 μM of pyrene was added to the tube, and an aqueous solution of cationic surfactant with various concentrations (5, 10, 25, 50, 100, 200, 300, 400, 500, 600, 700, 800, 900 and 1000 μM) was added followed by vortexing. The mixed solution was incubated at room temperature for 15 min. The emission spectrum was recorded for each solution from 350 to 450 nm after excitation with a wavelength of 334 nm (slit width was 1 nm for both excitation and emission). Similarly, samples were prepared in 1× PBS, and emission spectra were recorded for each sample. The data was plotted as I_1/I_3 ratio against concentration, I_1 and I_3 represent 373 and 384 nm, respectively.

2.3 *Preparation of micelles and hydrogel*

The 10 mM stock solution of cationic surfactant was prepared in double-distilled water by heating at 70°C for 1 h. Further, 1 ml of 1 mM solution was prepared in 1× PBS followed by heating at 80°C for 1 h and left for overnight at room temperature.

The hydrogels were prepared by sol–gel method. Briefly, the compounds were weighed and kept in respective glass vials followed by addition of 1 ml double-distilled water. The mixture was heated till clear solution appeared and left for overnight at ambient temperature. The formation of hydrogel was confirmed *via* dropping test by inverting the glass vial. Similarly, hydrogels were made in 1× PBS.

2.4 *Dynamic light scattering studies*

The prepared micelles were examined for their size and zeta potential using litesizer 500 (Anton Paar). The measurements were acquired in automatic mode and data presented as an average of 20 runs. The zeta potential of micelles was obtained by averaging the values from 30 runs with an effective voltage of 200 mV using disposable omega cuvettes.

2.5 *DNA retardation assay*

To assess the DNA binding affinity, 20 μl of the complex was prepared using 0.3 μg of plasmid DNA with cationic amphiphiles (in the absence and presence of PBS) at various charge ratios (+ve:−ve). The complexes were incubated for 30 min at ambient temperature and post-incubation mixed with tracking dye (xylene cyanol). The complexes were loaded on 0.8% agarose gel containing EtBr in their respective wells and electrophoresed in Tris acetate buffer for 30 min at 100 V for 45 min. The DNA bands were visualized on UV transilluminator in gel documentation system gel (Imagequant).

2.6 *Rheological studies*

Rheology studies of hydrogels were obtained on MCR92 instrument, Anton Paar equipped with a parallel plate with a radius of 12.5 mm. The hydrogels were prepared (in the presence and absence of PBS) 16 h prior to data acquisition, and viscoelastic properties were determined by simple amplitude sweep at a fixed frequency of 1.6 Hz.

2.7 *SAXS study of xerogel*

The xerogels of all hydrogels were prepared in a glass vial and dipped in liquid nitrogen for 10 min. Then, vials were kept for lyophilization, and a small fraction of xerogel was subjected to SAXS study using PANalytical Empyrean machine operating at 45 kV and 30 mA, using CuKα radiation ($\lambda = 1.5418$ Å) equipped with a PIXcel 3D detector.

2.8 *SEM analysis of xerogel*

To prepare xerogel for SEM analysis, hydrogels were transferred on glass coverslips and snap-frozen in liquid nitrogen followed by lyophilization. The coverslips were mounted on

stubs using double-sided carbon tape and were sputter-coated with gold. Images were acquired on Carl Zeiss merlin compact VP SEM at accelerating voltage of 1–5 kV.

2.9 *Cytotoxicity assay*

To assess the cytotoxicity of synthesized amphiphiles, three different cell lines were used viz. HDFA, HeLa and HEK293T cell lines. The 96-well plate for each cell line was prepared by seeding 10,000 cells in each well and incubated for 24 h with 5% CO_2, 95% humidity at 37°C. After getting the confluency of 70% in cell plate, the compounds were added at 0.5, 1, 10, 25 and 50 μM, followed by incubation for 24 h. Post-24 h treatment, solution of MTT reagent (1 mg ml^{-1} in PBS) was added and incubated for 4 h at 37°C, followed by complete aspiration of wells. The formazan crystals in the wells were dissolved by the addition of 100 μl DMSO, shaken gently to dissolve the crystals and absorbance was recorded in multiplate reader for each well. The cell viability was calculated as per the equation: cell viability (%) = [sample (A_{570})− blank (A_{570})]/[control (A_{570})−blank (A_{570})] × 100. The untreated cell was kept as control and considered as 100% cell viability.

2.10 *Haemolysis assay*

To evaluate haemocompatibility of cationic amphiphiles, the 4% haematocrit (100 μl) was prepared in saline and added to 96-well plate. Then, the amphiphiles including cetyl trimethyl ammonium bromide (CTAB) were added at the concentrations of 0.1, 1, 10, 25, 50 and 100 μM to their respective wells and incubated for 1 h at 37°C with continuous rotation at 100 rpm. The 0.1% Triton X-100, saline was taken as positive and negative controls, respectively. After 1 h incubation, the plate was centrifuged at 500 g for 10 min at room temperature. The 100 μl supernatant was carefully transferred to another plate, and absorbance was recorded at 540 nm. The haemolysis (%) was calculated using the equation: Haemolysis (%) = [sample (A_{540})−saline (A_{540})]/[Triton X-100 (A_{540})−saline (A_{540})] × 100.

3. Results and discussion

To examine the supramolecular self-assembly of small cationic amphiphiles consisting of benzene ring in hydrophobic tail, a two-step reaction has been employed to synthesize five novel molecules with different cationic head groups (scheme 1). The first step comprised of alkylation of 3-pentadecyl phenol with 1,2-dibromoethane to form a precursor molecule (1-(2-bromoethoxy)-3-pentadecyl benzene). Further, 1-(2-bromoethoxy)-3-pentadecyl benzene was subjected to synthesize desired quaternary salts after reaction with tertiary amine molecules, such as trimethyl amine (PEA), triethyl amine (PETE), pyridine (PEPy), *N*-methyl morpholine (PENM), *N*-methyl piperidine (PENP). These cationic amphiphiles have different head groups, where the quaternary ammonium group has alkyl groups (trimethyl and triethyl), aromatic (pyridine), cyclic (morpholino and piperidine). All the compounds we synthesized in good yield (50–90%) and characterized by ^{1}H-NMR and mass spectroscopy.

3.1 *Self-assembly of amphiphiles to form micelles in water and buffer*

3.1a *Determination of CMC (salting out effect)*: The CMC was determined for each amphiphile using pyrene as a fluorescent probe in the presence and absence of PBS [2]. The measured CMC values for PEA, PETE, PENM, PENP and PEPy in aqueous solution were 300, 100, 200, 25 and 800 μM, respectively (figure 1a). The PEA amphiphile, which is similar to CTAB showed lower CMC than CTAB surfactant, which is 0.9 mM [15]. The molecular structure of PEA consists benzene which provides additional π–π stacking interaction between hydrophobic tails of molecules. Thus, π–π stacking and hydrophobic interactions lead to the formation of supramolecular micellar structures at a lower concentration. Apart from the hydrophobic tail, head group also contributed to the formation of a much stable micellar structure at low concentrations. PETE is lower than PEA, due to more hydrophobic head groups. Similarly, PENP has lower CMC than PENM. The PEPy amphiphile showed CMC at 800 μM, higher than other four amphiphiles, which can be due to more electrostatic repulsion between delocalized cationic head groups.

Further, CMC was also determined in the presence of salts (PBS), which showed lower CMC in the absence of salts (figure 1b). The PEA, PETE, PENM and PENP amphiphiles showed CMC of 200, 50, 50 and 10 μM, respectively. The PEPy amphiphile formed crystals in the presence of PBS. The trend of reduction in CMC in the presence of salts compared to aqueous media can be attributed to the salting-out effect [14].

3.1b *Size and charges of self-assembled micelles*: Particle size and zeta potential of self-assembled cationic amphiphile were determined using dynamic light scattering. The hydrodynamic diameter of self-assembled micelles was measured in the presence of salt. All micelles were showed size <100 nm (figure 2a), but the PEPy formed crystal in the presence of PBS. In the absence of salt, particle size was not stable (data not included), because of dynamic nature of micelles and due to formation of elongated WM structure. As proposed, amphiphiles have cationic head groups, zeta potential or surface charge of the micellar structures were determined. In figure 2b, all amphiphilic nanostructures showed positive zeta potential in the absence of salt, while in the presence of salt, masking of charge was observed. Due to the presence of salts, the thickness of the stern layer of micelles got reduced, which leads to a decrease in surface charge or zeta potential [16]. Thus, reduction of charge in the presence of salt was in agreement with reported literature [14]. Further, to confirm the masking of charge in the presence of

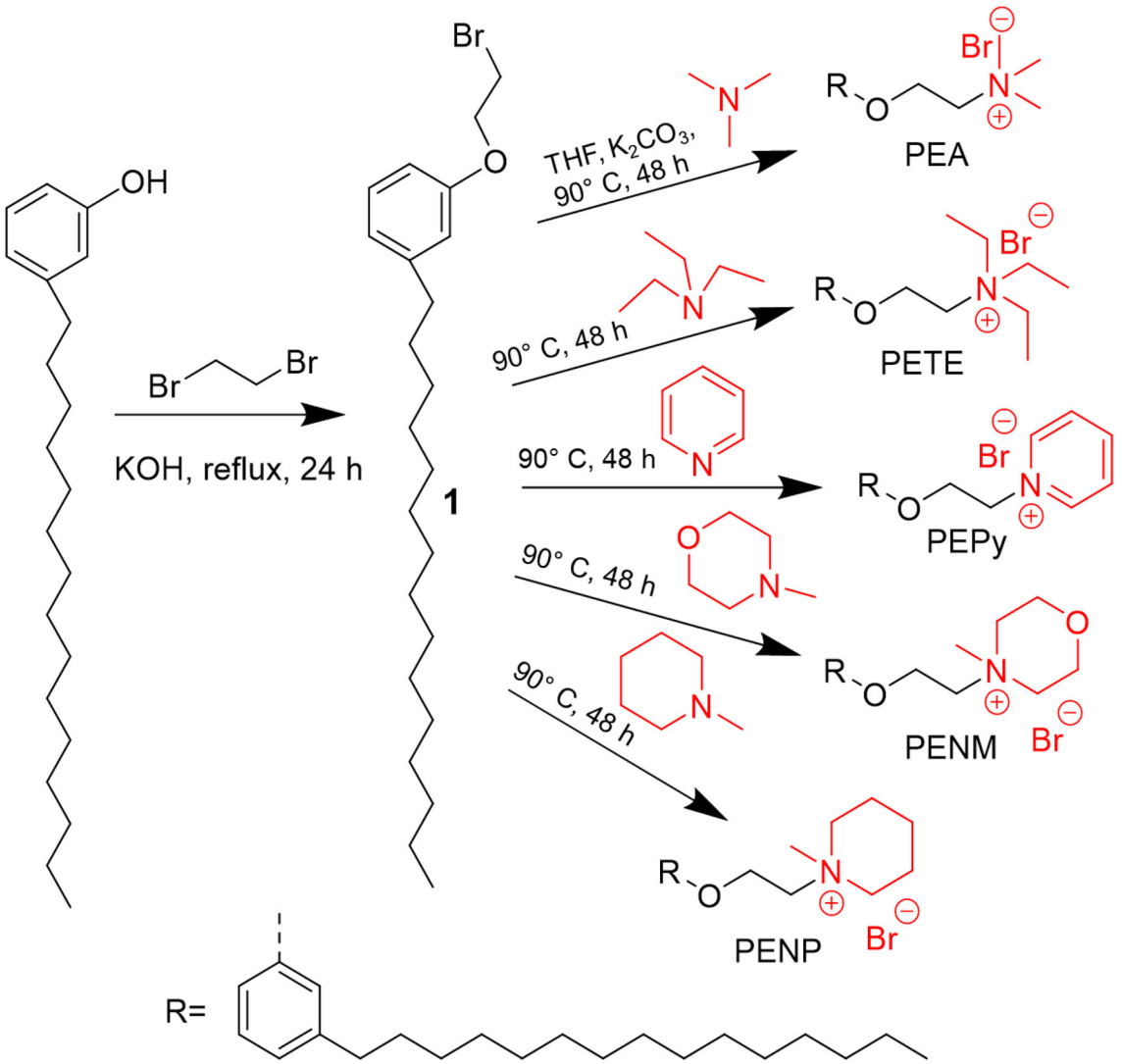

Scheme 1. Synthesis of designed cationic amphiphiles.

PBS, DNA retardation was done at various charge ratios. The micelles prepared in the absence of PBS were able to retard the DNA at charge ratio (+ve/-ve) of 3:1 (PEA), 8:1 (PETE), 5:1 (PENM), 10:1 (PENP) and 5:1 (PEPy) (figure 2c). While, DNA retardation with amphiphiles in the presence of PBS was showing retardation at a charge ratio of 5:1 (PEA), 10:1 (PETE), 10:1 (PENM), 15:1 (PENP) and 10:1 (PEPy). Hence, in the presence of salts, there is a significant reduction in the surface charge occurred.

3.2 *Formation of self-assembled hydrogels in water and buffer*

3.2a *Measuring CGC and rheology of hydrogels*: Interestingly, the cationic amphiphiles showed gelation in deionized water at higher concentration after heating and cooling cycles. The critical gelation concentrations (CGC) of PEA, PETE, PENM, PENP and PEPy were found to be 3, 5, 8, 10 and 5%, respectively (table 1). Moreover, they formed hydrogels in the presence of PBS as well, except PEPy, which formed a thick emulsion in PBS. All the hydrogels were thermo-reversible in nature (in the presence and absence of salt). The appearance of hydrogel was clear except PENP showed yellowish coloured gel. The melting temperature was also determined by visual observation method, where the temperature was noted when the whole gel melted down. All hydrogels were made using 10% (w/v) of amphiphile in aqueous media to measure the gel melting temperature. The melting temperatures of PEA, PETE, PENM, PENP and PEPy were found to be 80, 48, 70, 48 and 66°C, respectively. The melting temperature of hydrogel completely correlates with rheology data showing high strength/elasticity material, which needs more heat energy to convert from gel to sol.

The rheological studies were conducted for all hydrogels prepared using a parallel plate, keeping a constant frequency

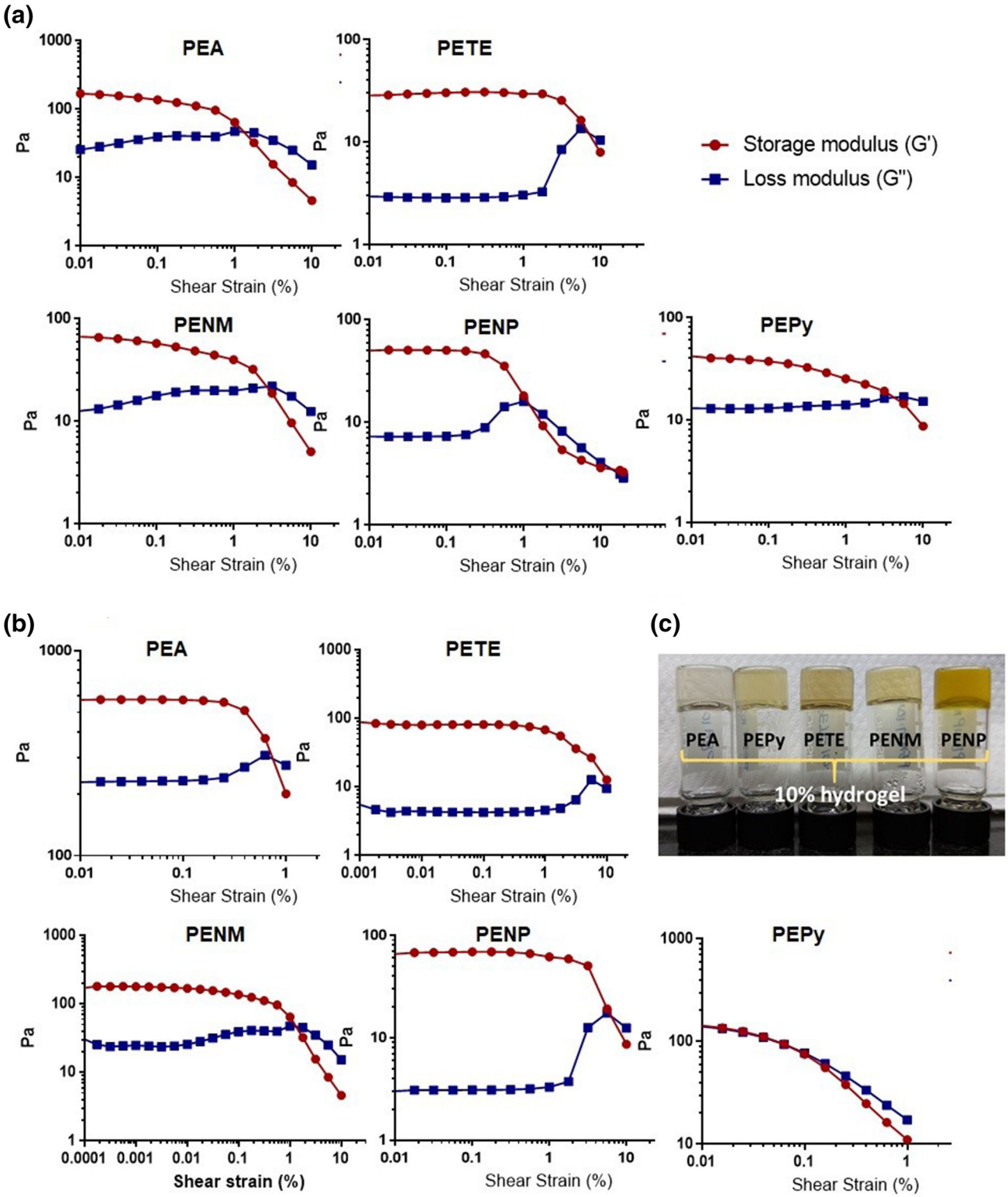

Figure 1. CMC of cationic amphiphiles (**a**) in the absence of PBS and (**b**) in the presence of PBS.

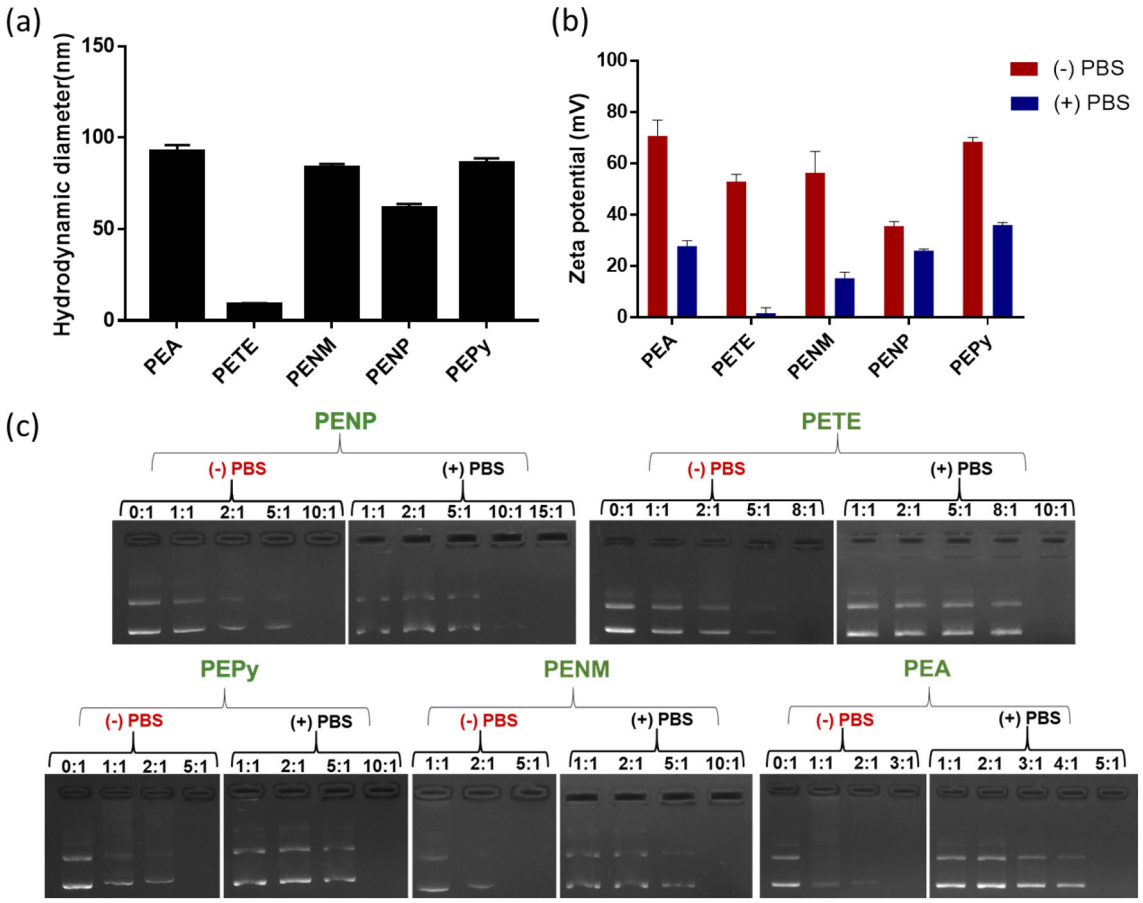

Figure 2. (**a**) Particle size of amphiphiles (1 mM) in PBS, (**b**) zeta potential of cationic amphiphile (1 mM) in the presence and absence of PBS and (**c**) DNA retardation of each amphiphile in the presence and absence of PBS.

Table 1. Critical gelation concentration (CGC) and melting temperature of gels in the absence of PBS.

Amphiphile	CGC (%), w/v	Melting temperature, T_m (°C) 10% w/v
PEA	3	80
PETE	5	48
PENM	8	70
PENP	10	48
PEPy	5	66

Table 2. Rheological properties of cationic amphiphiles.

	Storage modulus, G' (Pa)		Loss modulus, G'' (Pa)		G'/G''	
Gels (10%)	(−) PBS	(+) PBS	(−) PBS	(+) PBS	(−) PBS	(+) PBS
PEA	172	588.7	30.389	288.29	5.65	2.04
PETE	26.4	99	10.06	6.97	2.62	14.2
PENM	78	172.3	16.14	30.38	4.83	5.67
PENP	49.95	50.34	7.16	6.5	6.97	7.74
PEPy	42.56	DNG	15.05	DNG	2.82	NA

DNG: did not gel.

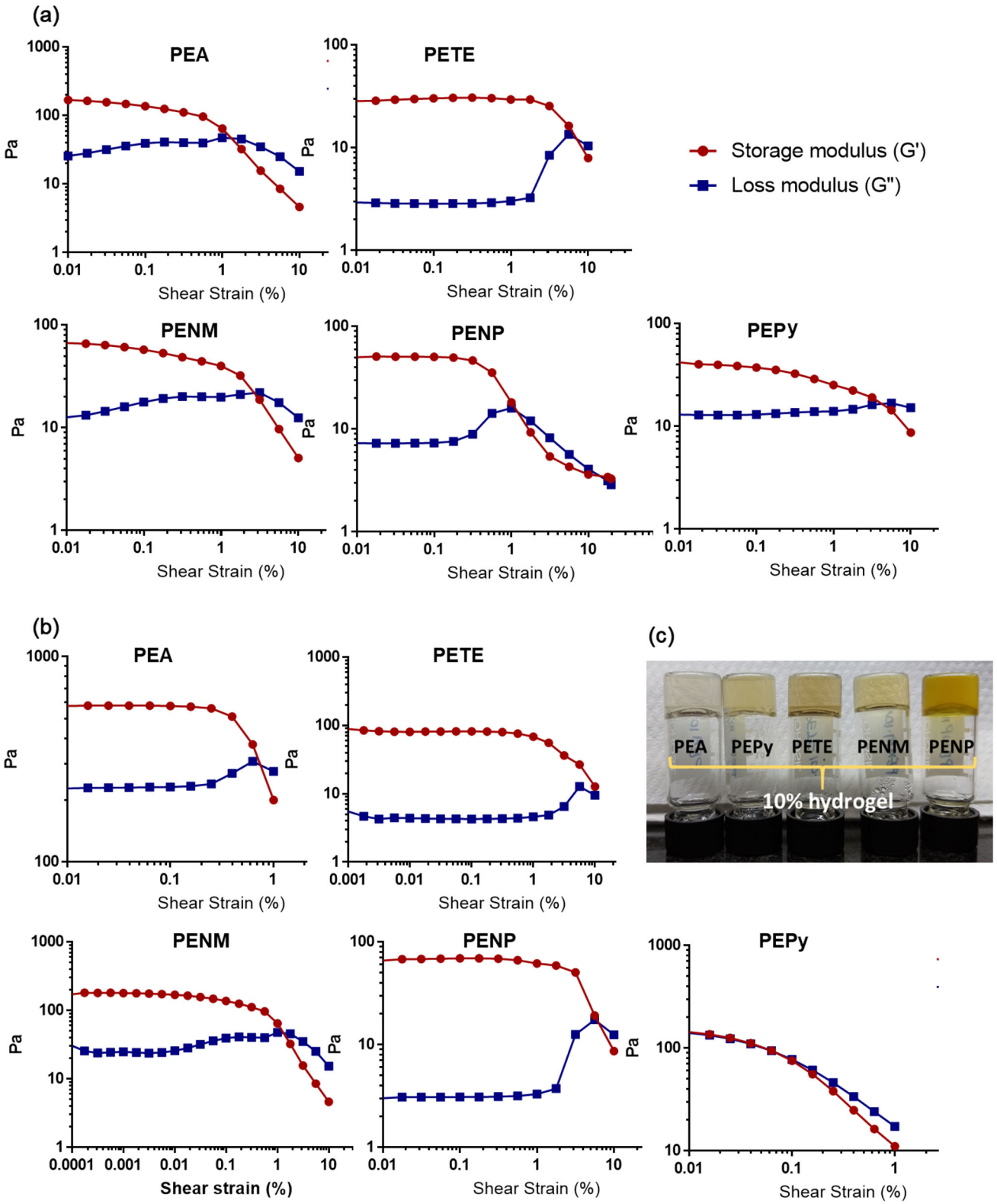

Figure 3. Amplitude sweep for all the gels (10%, w/v) at constant frequency of 1.6 Hz: (**a**) in the absence of PBS, (**b**) in the presence of PBS and (**c**) image of cationic hydrogels prepared in the absence of PBS.

of 1.6 Hz. According to the data in table 2, the storage modulus (G') for all the amphiphiles was higher than their respective loss modulus (G''), which confirms the formation of hydrogels. In figure 3 and table 2, the storage modulus (G') of these amphiphilic hydrogels were in the range of 26.4–172 Pa (in the absence of PBS) and 50.34–588.7 Pa (in the presence of PBS). The increase in storage modulus is directly proportional to the elasticity and strength of hydrogel. Thus, in the presence of PBS, hydrogels were found to be more elastic. The behaviour can be explained on the basis of masking of cationic charge by salt ions, which enhances hydrophobic interaction between the molecules [17]. Moreover, G'/G'' ratios of all hydrogels were in the range of 2–14.2; hence, these amphiphiles form very soft hydrogels with viscoelastic property. The phenomena of gelation can be explained *via* the formation of worm-like micelles at higher surfactant concentration, which has been extensively demonstrated in the literature using cationic surfactants [18]. The molecular structure of all the amphiphiles did not have any form of H-bond donor or acceptor such as (–NH_2), hydroxyl (–OH) and carboxylic acid (–COOH) groups, unlike small peptide-based nanostructure and others [19,20]. In this study, self-assembly was only driven by hydrophobic and π–π stacking interaction between the molecules, which are weaker non-covalent bonds as compared to H-bonding, resulted in loose packing of macroscopic structures (soft gels).

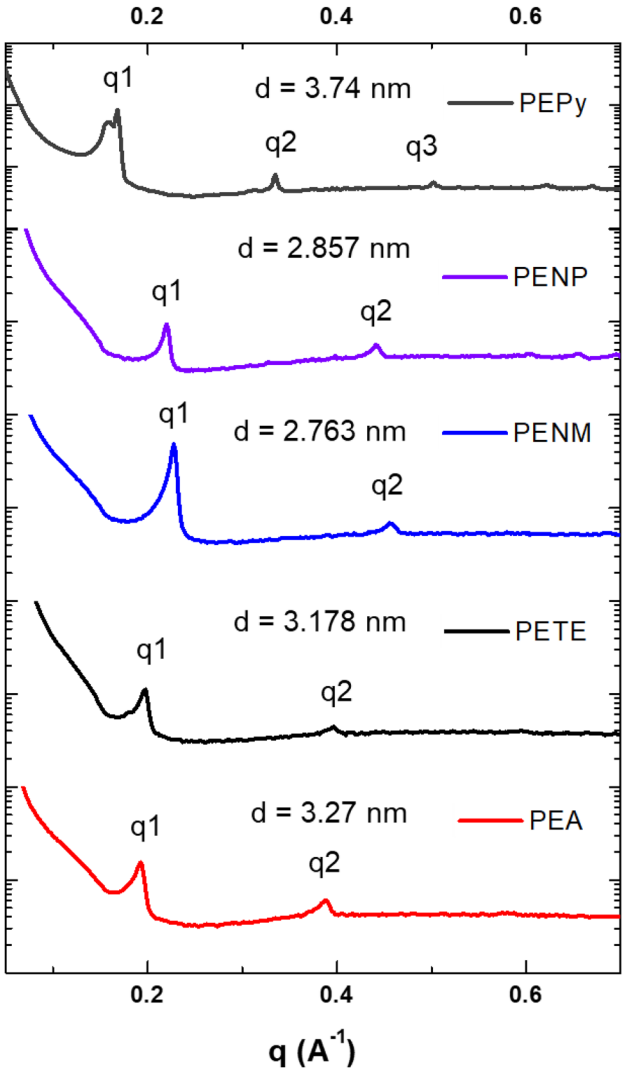

Figure 4. SAXS data of xerogel from all cationic amphiphiles in the absence of PBS.

3.2b *SAXS studies*: To determine the order of self-assembly mediated by the molecules to form the hydrogel, SAXS study was employed. The hydrogels made in the absence of PBS were snap-frozen and lyophilized to form xerogels for each amphiphile. Data in figure 4 and table 3 suggests that the peaks at scattering vector q1, q2 and q3 appeared at regular intervals at a ratio of 1:2:3 (q1:q2:q3) for PEA, PETE, PENM and PENP, while PEPy was showing up to q4, which strongly advocates for the formation of higher-ordered lamellar structures. The lamellar structure length was calculated from the Bragg's equation and was found to be 3.27, 3.187, 2.763, 2.857 and 3.74 nm for PEA, PETE, PENM, PENP and PEPy, respectively. The scattering vector (q) showed regular peaks at definite intervals for each amphiphilic xerogels, which strongly suggests a lamellar arrangement of molecules to form hydrogels. The supramolecular structures showed lamellar structures and indicated the formation of worm-like micelles at higher concentration to form viscoelastic hydrogels. The worm-like micelles entangle with each other, and form highly branched networks or mesh-kind of structures, which was observed under the SEM images (figure 5).

Table 3. Scattering vectors for each cationic amphiphile and supramolecular structures length.

Cationic amphiphile	q1 (A^{-1})	q2 (A^{-1})	q3 (A^{-1})	q1:q2:q3	Supramolecular structure (d, nm)
PEPy	0.168047	0.335108	0.502028	1:2:3	Lamellar (3.74)
PENP	0.220033	0.440845	0.657632	1:2:3	Lamellar (2.857)
PENM	0.227458	0.455679	0.68724	1:2:3	Lamellar (2.763)
PETE	0.197754	0.396332	0.581709	1:2:3	Lamellar (3.178)
PEA	0.192184	0.388912	0.583561	1:2:3	Lamellar (3.27)

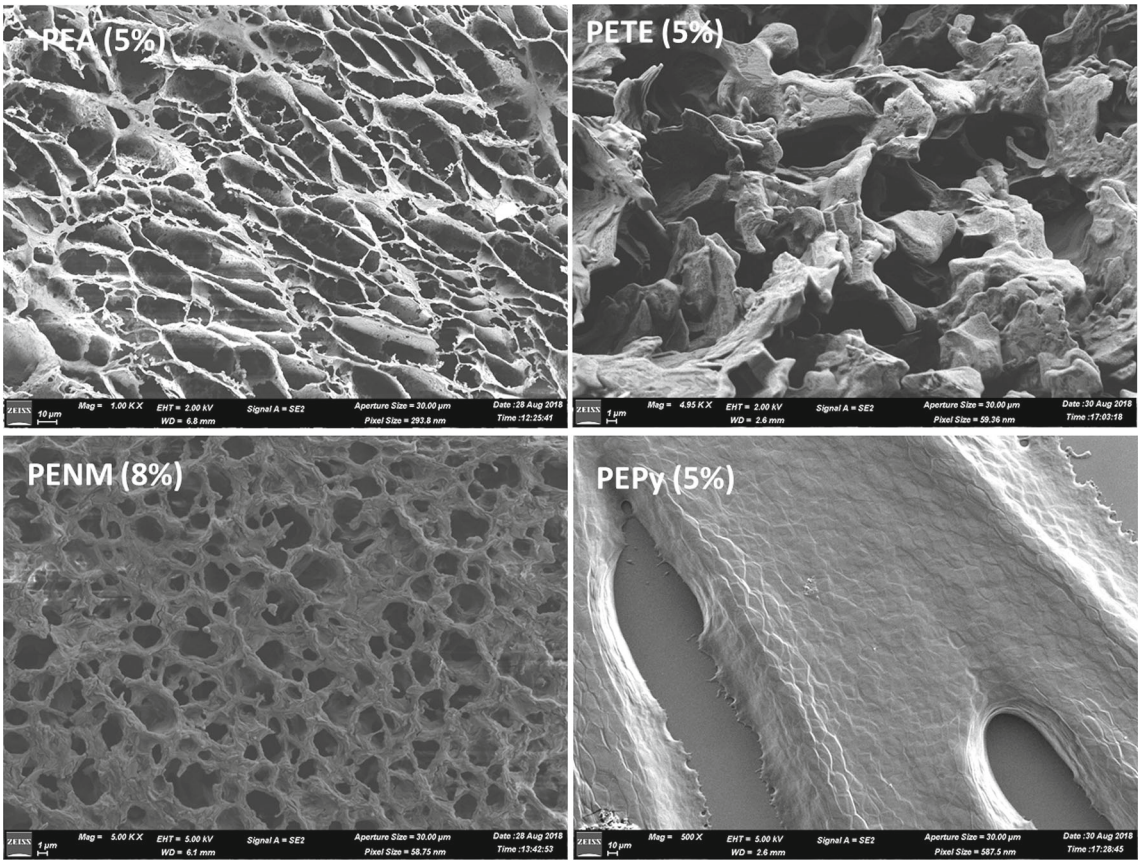

Figure 5. SEM micrographs of xerogels prepared using self-assembly of cationic amphiphiles in the absence of PBS.

3.2c *Morphology study using SEM*: Xerogels were evaluated for SEM micrographs and revealed mesh-like structures, which also supports the SAXS data for the formation of worm-like supramolecular micellar structures. In figure 5, PEA, PETE and PENM showed mesh-like structures, where worm-like micellar structures entangled with each other to form viscoelastic hydrogels. The PEPy was forming high-ordered stacked lamellar structures, which completely correlate with SAXS data of high-order lamellar arrangement (figure 4).

3.3 *Solubilization of hydrophobic drugs*

The cationic amphiphiles were evaluated for solubilizing highly hydrophobic drugs. In the present study, curcumin was chosen as a model hydrophobic molecule with a solubility of 60 μg ml^{-1} in water [21]. Among all the amphiphiles, the PEA showed higher solubilization efficacy of around 4.9 mg of curcumin in 1 ml of PEA (10 mM), while CTAB (10 mM, 1 ml) has solubilized 1.45 mg of curcumin (table 4). The other amphiphiles showed higher solubilization than CTAB except for PEPy, only 0.56 mg of curcumin in 1 ml of PEPy (10 mM). The lower solubilization efficacy can be explained on the basis of higher CMC value of PEPy (0.8 mM) among other synthesized amphiphiles, a higher number of molecules required to reduce the surface tension and solubilize the hydrophobic drug. Moreover, PEPy has greater lamellar structure length as found from SAXS study, which tells there is a loose packing between the molecules. Hence, weaker intermolecular forces to entrap hydrophobic curcumin molecules.

3.4 *Biocompatibility of cationic amphiphiles*

Haemolysis and cell viability assays were used to investigate the biocompatibility of all synthesized cationic amphiphiles. The cell viability of amphiphiles was evaluated using three cell lines viz. HEK293, HeLa and HDFA after incubation for 24 h (figure 6). The cell viability varied with different cell types, in HEK cell line at 10 μM was found to be up to 60–70%, while at a higher concentration showed significant toxicity above 25 μM. In HeLa and HDFA cell lines, amphiphiles showed cell viability up to 40–50% at 10 μM and at higher concentration, significantly dropped. Among all, PEA and PENM showed the highest cell viability (75%) at 25 μM in HEK cell line. The results were in complete agreement with the reported literature, which also shows similar toxicity profile of other cationic amphiphiles below their CMC values [22].

Haemolysis assay was also determined for all cationic amphiphiles and CTAB. The amphiphiles showed low haemolytic activity as compared to CTAB, at 10 μM CTAB was

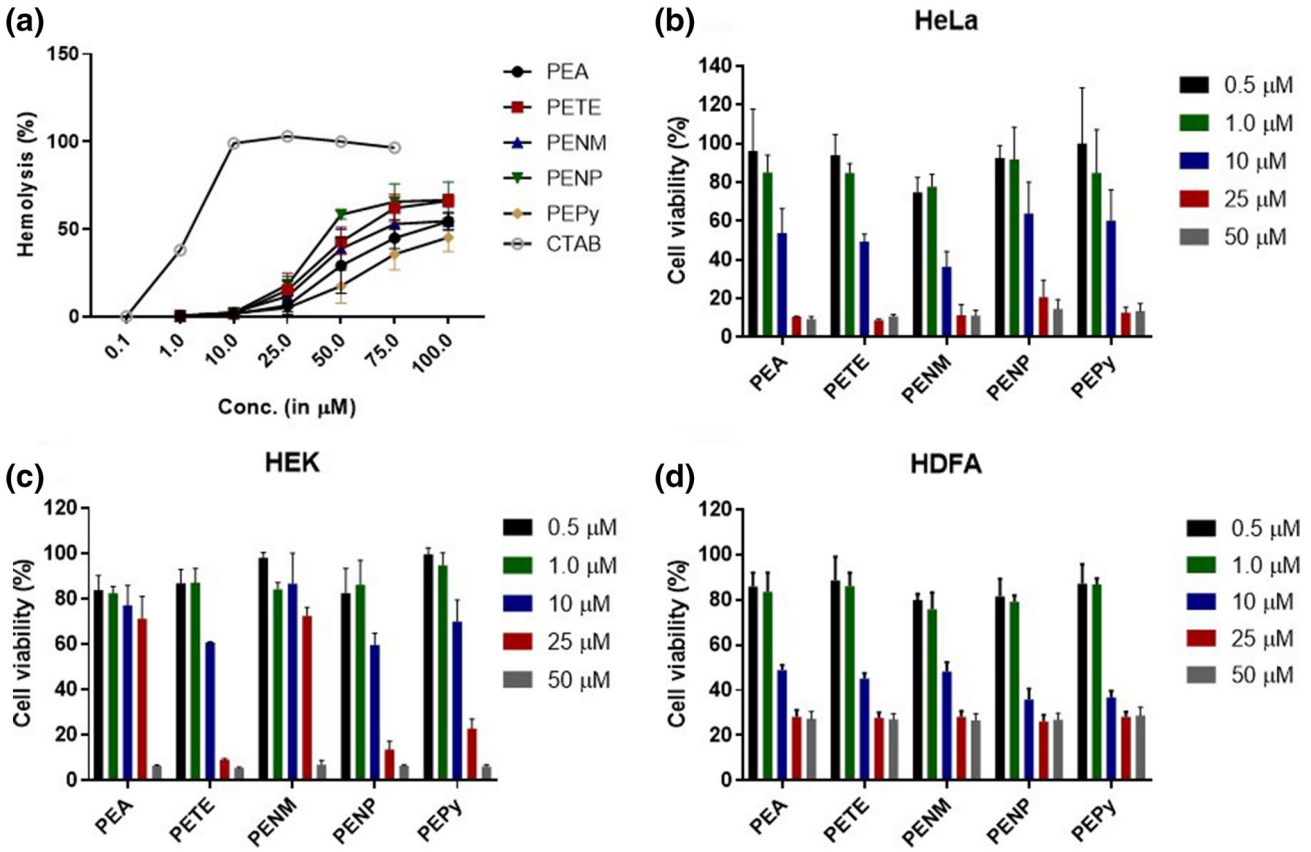

Figure 6. Biocompatibility assay for the cationic amphiphiles. (**a**) Haemolysis assay and cell viability on (**b**) HeLa, (**c**) HEK293 and (**d**) HDFA cell lines, respectively.

Table 4. Solubilization of curcumin in the presence of cationic amphiphiles.

Amphiphile (1 ml, 10 mM)	Solubilized curcumin (mg) ± SD
CTAB	1.45 ± 0.2
PEA	4.9 ± 0.41
PETE	1.86 ± 0.15
PENM	2.12 ± 0.13
PENP	2.1 ± 0.059
PEPy	0.55 ± 0.05

haemolysing the RBCs, while around 100 μM amphiphiles showed around 70% haemolysis. Thus, the series of amphiphiles have low haemolytic activity and PEPy showed lowest haemolytic activity at 100 μM, which was found to be around 50%.

4. Conclusions

In this study, we have shown a series of cationic amphiphiles with 3-pentadecyl benzene as a hydrophobic tail for π–π stacking and hydrophobic interactions, which lead to the formation of self-assembled micellar structures in aqueous and PBS buffer media. Owing to the salting-out effect, the amphiphiles formed stable nanoparticles in the presence of salts. On the contrary, these amphiphiles formed unstable nanoparticles in aqueous media without salts. At a higher concentration, these amphiphiles formed hydrogels and shown viscoelastic nature. At molecular level, SAXS studies demonstrated the lamellar arrangement of molecules to form macroscale structures like hydrogels. Based on the present study, the effect of position isomer on the benzene ring with aliphatic chains can be carefully studied to get a better understanding in designing of self-assembled structures and their potential biomedical applications.

Acknowledgements

We thank Prof S Ramakrishnan, Department of Inorganic and Physical Chemistry, Indian Institute of Science for SAXS Studies, Central Imaging and Flow Facility (CIFF) at NCBS/inStem, Bangalore, for SEM micrographs. We thank NMR facility at NCBS/inStem. OS thanks ICMR for the award of senior research fellowship (SRF) to carry out the research project. HSR thanks the Indian Academy of Sciences for the Summer Research Fellowship Program. SK thanks

Department of Biotechnology-Research associate (DBT-RA) fellowship. PKV thanks inStem, Department of Biotechnology, Govt. of India, for core funding.

References

[1] Yang J 2002 *Curr. Opin. Colloid Interface Sci.* **7** 276
[2] Wang Y, Han Y, Huang X, Cao M and Wang Y 2008 *J. Colloid Interface Sci.* **319** 534
[3] Bhattacharya S and Subramanian M 2002 *Tetrahedron Lett.* **43** 4203
[4] Roszak K Z, Torcivia S L, Hamill K M, Hill A R, Radloff K R, Crizer D M *et al* 2009 *J. Colloid Interface Sci.* **331** 560
[5] Song B, Wei H, Wang Z, Zhang X, Smet M and Dehaen W 2007 *Adv. Mater.* **19** 416
[6] Chu Z, Dreiss C A and Feng Y 2013 *Chem. Soc. Rev.* **42** 7174
[7] Cates M E and Candau S J 1990 *J. Phys. Condens. Matter* **2** 6869
[8] Raghavan S R and Feng Y 2017 *RSC Soft Matter* **2017** 9
[9] Jiang G, Jiang Q, Sun Y, Liu P, Zhang Z, Ni X *et al* 2017 *Energy Fuels* **31** 4780
[10] Ezrahi S, Tuval E and Aserin A 2006 *Adv. Colloid Interface Sci.* **128–130** 77
[11] Raghavan S R and Kaler E W 2001 *Solutions* **18** 300
[12] Zhang Y, Guo Z, Zhang J, Feng Y, Wang B and Wang J 2011 *Prog. Chem.* **23** 2012
[13] De S, Aswal V K and Ramakrishnan S 2010 *Langmuir* **26** 17882
[14] Ren Z H 2015 *Ind. Eng. Chem. Res.* **54** 9683
[15] Li W, Zhang M, Zhang J and Han Y 2006 *Front. Chem. China* **1** 438
[16] Brown M A, Goel A and Abbas Z 2016 *Angew. Chemie - Int. Ed.* **55** 3790
[17] Schubert B A, Kaler E W and Wagner N J 2003 *Langmuir* **19** 4079
[18] Nakama Y 2017 *Cosmetic science and technology: theoretical principles and applications* **2017** 231
[19] Du X, Zhou J, Shi J and Xu B 2015 *Chem. Rev.* **115** 13165
[20] Mahato M, Arora V, Pathak R, Gautam H K and Sharma A K 2012 *Mol. Biosyst.* **8** 1742
[21] Shin G H, Li J, Cho J H, Kim J T and Park H J 2016 *J. Food Sci.* **81** 494
[22] Inacio A S, Mesquita K A, Baptista M, Ramalho-Santos J, Vaz W L C and Vieira O V 2011 *PLoS One* **6** 19850